https://doi.org/10.5194/egusphere-2026-130
Preprint. Discussion started: 24 March 2026
© Author(s) 2026. CC BY 4.0 License.

Simulation of sliding deadwood logs in mountain forests: towards a quantitative hazard assessment

Joël Borner[1,2,3], Peter Bebi[1,2], Leon J. Bührle[1,2,4], Adrian Ringenbach[1,2], and Remco Leine[5]

[1]WSL Institute for Snow and Avalanche Research SLF, Davos, Switzerland
[2]Climate change, Extreme events and natural hazards in mountain regions Research Centre CERC, Davos, Switzerland
[3]Institute for Geotechnical Engineering, ETH Zurich, Zurich, Switzerland
[4]Department of Natural Hazards, Austrian Research Centre for Forests (BFW), Innsbruck, Austria
[5]Institute for Nonlinear Mechanics, University of Stuttgart, Stuttgart, Germany

Correspondence: Joël Borner (joel.borner@slf.ch)

Abstract. Deadwood is an integral component of mountain forests, supporting biodiversity and contributing to protection against gravitational hazards. However, under specific conditions, deadwood may itself become a hazard when mobilised and transported downslope. Although sliding logs have been repeatedly observed in steep forests, a quantitative framework to assess their hazard potential has so far been lacking. We present a physics-based model to simulate the motion and runout of sliding deadwood logs in complex terrain. The model extends an existing rockfall simulation framework based on nonsmooth rigid-body dynamics with hard contact laws and Coulomb friction, explicitly representing deadwood log geometries and interactions with terrain, standing trees, and protective structures. Model calibration and evaluation are performed using two recent Swiss case studies in which deadwood logs up to 35 m in length travelled several hundred metres in a single rapid descent and impacted infrastructure. Simulations indicate that sliding deadwood hazard is favoured by very steep slopes >35°, wet surface conditions, and a narrow decay-stage window characterised by the loss of bark and branches to reduce sliding friction while still retaining sufficient structural strength. Sliding trajectories are strongly controlled by micro-topography, with preferential paths along gullies, while standing trees limit downslope propagation but increase lateral spread through repeated deflections. The proposed model highlights the importance of adaptive forest management in mountain forests and provides a quantitative basis for optimising the balance between the protective and hazardous roles of deadwood.

1 Introduction

Mountain forests provide cost-effective and natural protection of civil infrastructure against natural hazards in mountain regions (Moos et al., 2017; Getzner et al., 2017; Olschewski et al., 2012). The amount of deadwood in Swiss mountain forests has doubled during the last three decades, from 17 m^3 ha^{-1} in 1995 (Abegg et al., 2023b) to 35 m^3 ha^{-1} today (Abegg et al., 2023a). Under future climatic conditions, the amount of standing and lying deadwood are expected to increase as a result of enhanced drought-induced tree mortality and intensifying natural disturbance regimes (Seidl et al., 2017). While the influence of deadwood on biodiversity (Gossner et al., 2016; Plath and Fischer, 2024), regeneration processes (Marangon et al., 2024), and other ecological functions (Edelmann et al., 2023; Mayer et al., 2022) is relatively well investigated, its effects on protection

https://doi.org/10.5194/egusphere-2026-130
Preprint. Discussion started: 24 March 2026
© Author(s) 2026. CC BY 4.0 License.

against natural hazards are less studied and often debated (Fuhr et al., 2015). The few studies conducted so far suggest that deadwood can reduce the risk of avalanches (Caduff et al., 2022; Feistl et al., 2014; Rammig et al., 2007; Schönenberger et al., 2005) and rockfalls (Bourrier et al., 2012; Ringenbach et al., 2023; Costa et al., 2021) in the short to medium term. There are, however, also potential risks associated with leaving deadwood after natural disturbances, including subsequent bark beetle infestations in spruce-dominated forests (Stadelmann et al., 2014), the secondary triggering of rockfall after advanced wood decay (Ringenbach et al., 2022a), and blockage of streams increasing the risk of debris flows and floods (Rackelmann et al., 2023). Moving deadwood can also become a hazard itself, making it crucial to understand the conditions under which this occurs. Such risks highlight the need for an integral view in making general recommendations for deadwood management in mountain forests. In order to better assess both the protective effect and hazard potential of deadwood, information on its spatial distribution and potential downward movements must be known. Various processes drive deadwood movement across a range of spatial scales (Harmon et al., 1986). At the broadest scales, rivers and floods transport deadwood up to several kilometres (May and Gresswell, 2003). At the finest scales, deadwood moves through gradual processes (Bebi et al., 2015) or when snags fall (Oberle et al., 2016). In between, on the slope scale, deadwood may be transported by landslides, surface run-off, or avalanches (Kemper and Scamardo, 2023).

This paper is motivated by recent events in Switzerland in which deadwood without bark and branches was mobilised and travelled several hundred metres in a single rapid descent, causing damage to infrastructure. We focus thereby on deadwood as a direct form of natural hazard when it is mobilised and slides down a steep slope. To date, the mechanics of such rapid sliding events have not been quantified, and no modelling framework exists to describe how mobilised deadwood moves on steep slopes. As the downslope motion of deadwood shares key mechanical characteristics with rockfall, including gravity-driven acceleration, impact, sliding, and deflection by obstacles, existing rockfall modelling frameworks appear in principle to be an ideal framework for such simulations. However, from a modelling perspective, sliding deadwood poses specific requirements that are not fulfilled by most existing rockfall models, including the ability to represent sliding motion, simulate arbitrary three-dimensional object shapes, and explicitly model interactions with individual standing trees. These limitations motivate the use and adaptation of a physically based rigid-body framework in this study. We therefore adapt the physical approach of RAMMS::Rockfall (Christen et al., 2014) introduced by Leine et al. (2014), using non-smooth, rigid-body mechanics in combination with hard contact laws and Coulomb friction. We calibrate and validate the model based on case studies of recent sliding deadwood events, discuss the factors favouring mobilisation and critical predispositions related to deadwood and terrain conditions, and finally assess the relevance of sliding deadwood logs in the context of other natural hazards as well as their implications for mountain forest management.

2 Sliding deadwood events

2.1 Klosters, Graubünden (CH)

Gruobenwald (46.89025° N; 9.85585° E; 1050–1300 m a.s.l) is a roughly 35° steep beech spruce forest near Klosters, Switzerland (see Fig. 1). Due to the steep slope, the cliffs above the forest, which reach heights of up to 130 m, and the exposed

https://doi.org/10.5194/egusphere-2026-130
Preprint. Discussion started: 24 March 2026
© Author(s) 2026. CC BY 4.0 License.

infrastructure (road of national importance, railway, residential area), rockfall hazards have been an ongoing issue for many years. As the outdated protective structures needed to be replaced, the construction of new measures started in 2022, consisting of 650 m of reinforced earth dams with a capacity of 5000 kJ and 400 m of rockfall barriers with a capacity of 2000 kJ. There are many dead trees, so called snags, without bark and branches, but which are still standing. In June 2022, a storm with heavy rainfall and wind caused a dead tree to fall and slide approximately 120 m down the slope until it came to rest on the national road (Fig. 1c). The mobilised tree had an approximate diameter at breast height DBH = 75 cm and a stem height h_S = 30 m. Two days later, another deadwood log of similar dimensions slid down the slope and came to rest in a wooden palisade next to a building (see Fig. 1b). Due to these two incidents and the associated danger to the construction site, the local forestry operators decided to cut down potentially dangerous snags without bark and branches and to transport them down to the valley by helicopter. During this operation, two more logs were mobilised after being cut down, slid down the slope and came to rest on the road or hiking trail, respectively. After completion of the intervention, there were no more recorded events as of December 2025.

https://doi.org/10.5194/egusphere-2026-130
Preprint. Discussion started: 24 March 2026
© Author(s) 2026. CC BY 4.0 License.

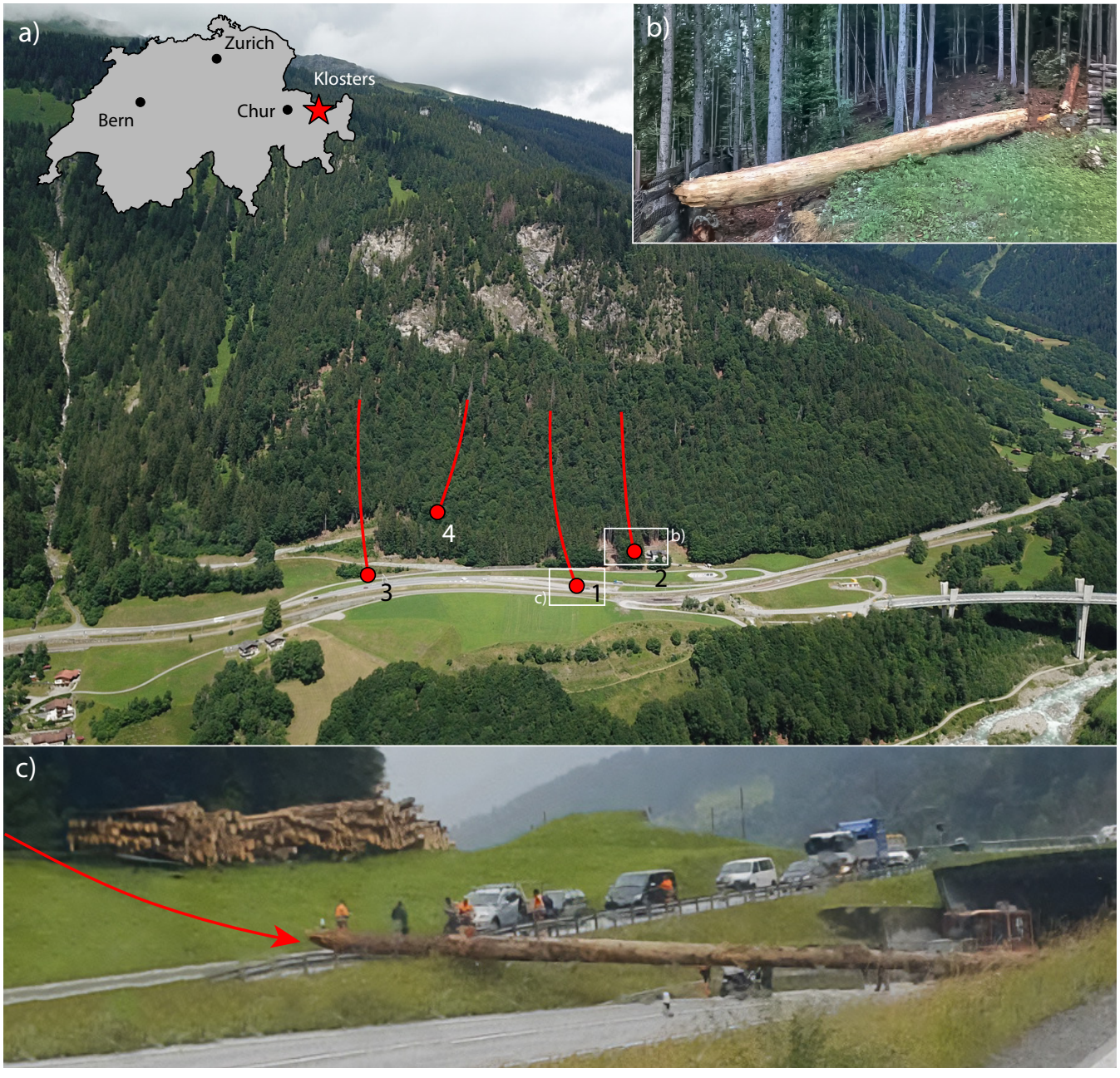

Figure 1. The four 2022 events in Gruobenwald, Klosters (CH). a) Overview of Gruobenwald, including endangered residential area, road and railway. The trajectories and deposition points of the four events are shown qualitatively. Photograph by AWN GR. b) Deposition of event 2 in a wooden palisade next to a house. c) Deposition of event 1 on the road. Photograph credit for b) and c): Flurin Wehrli.

https://doi.org/10.5194/egusphere-2026-130
Preprint. Discussion started: 24 March 2026
© Author(s) 2026. CC BY 4.0 License.

2.2 Rothenbrunnen, Graubünden (CH)

Plattawald (46.77072° N; 9.41829° E; 600–1000 m a.s.l) is a mountain forest near Rothenbrunnen, Switzerland. The average slope gradient is 35–40°, and a road and railway line run along the foot of the slope. There are numerous cases of rockfall and sliding deadwood on this slope, which cause only minor damage as the rocks and deadwood are caught by a series of rockfall barriers above the road. In February 2022, a tree without bark and branches was mobilised, slid down approximately 200 m in altitude and came to rest in the valley-side guardrail of the road, blocking both the road and the railway. It is unclear whether the mobilised tree was initially standing or lying. Due to a thin layer of snow on the day of the incident, the tracks of the sliding log were clearly visible and were documented by the local forestry operations. As the section of road where the log was deposited is protected by a 3.5 m high rockfall barrier and no traces were found in the immediate vicinity of the barrier, the log must have jumped over the barrier. This claim is reinforced by the fact that the last traces were found on a small terrace about 20 m above the barrier, where the log was presumably launched into the air. The next tracks were then found on the retaining wall next to the road.

3 Sliding deadwood model with Coulomb friction

For the modelling and simulation of the trajectories of sliding deadwood, we apply the theory and methods of nonsmooth dynamics (Acary and Brogliato, 2008; Leine and van de Wouw, 2008), encompassing rigid-body mechanics coupled with hard contact laws and Coulomb friction. Hereto, we adopt the framework for rockfall modelling introduced by Leine et al. (2014), which provides the mathematical basis for the kinematics, contact formulation, Coulomb friction, and Newton-type impact law, and we adapt this framework to the modelling of sliding deadwood. The deadwood is modelled as rigid, convex polytopes in the shape of a truncated cone, representing straight, radially symmetrical logs with a smooth surface (see Fig. 2b). The properties of these logs include a DBH, simplified as the base diameter of the truncated cone, a stem height h_S (also referred to as log length when lying) and a density ρ_S. The top diameter of the truncated cone is approximated with 0.5 DBH.

3.1 Coordinate frames and generalised coordinates

Following Leine et al. (2014), the motion of the log is described using two coordinate frames. The inertial frame I is fixed in space and anchored at the origin O, which is defined at the origin of the digital elevation model (DEM). The axes $\boldsymbol{e}_x^I$ and $\boldsymbol{e}_y^I$ span the horizontal plane, while the axis $\boldsymbol{e}_z^I$ extends along the vertical, counter-gravitational direction. The body-fixed frame K is attached to the centre of mass S of the log. The three axes $\boldsymbol{e}_x^K$, $\boldsymbol{e}_y^K$ and $\boldsymbol{e}_z^K$ are along the log's principal axes of inertia. The minor principal axis of inertia for a truncated cone lies in its longitudinal direction, which we define as $\boldsymbol{e}_z^K$. The two coordinate systems, their origins and axes are shown in Fig. 2a.

At any time t, the position and orientation of the log, modelled as a rigid body, is given by the generalised coordinates $\boldsymbol{q}$:

$$\boldsymbol{q} := \begin{pmatrix} {}_I\boldsymbol{r}_{OS} \\ \boldsymbol{p}_{IK} \end{pmatrix} \in \mathbb{R}^7, \tag{1}$$

https://doi.org/10.5194/egusphere-2026-130
Preprint. Discussion started: 24 March 2026
© Author(s) 2026. CC BY 4.0 License.

where ${}_I\boldsymbol{r}_{OS}$ is the position vector from the origin O to the centre of mass S, expressed in the inertial frame I, and $\boldsymbol{p}_{IK} = (e_0 \ \boldsymbol{e}^T)^T \in \mathbb{R}^4$ is a unit quaternion describing the orientation of the log. A linear mapping of $\dot{\boldsymbol{q}}$ leads to the dimension-reduced, generalised velocities $\boldsymbol{u}$:

$$\boldsymbol{u} = \mathbf{F}(\boldsymbol{p}_{IK})\,\dot{\boldsymbol{q}} := \begin{pmatrix} {}_I\boldsymbol{v}_S \\ {}_K\boldsymbol{\Omega} \end{pmatrix} \in \mathbb{R}^6, \qquad \mathbf{F}(\boldsymbol{p}_{IK}) = \begin{bmatrix} \mathbf{I}_{3\times3} & 0 \\ 0 & -\frac{1}{2}\boldsymbol{e}^T \\ 0 & \frac{1}{2}e_0\mathbf{I} + \frac{1}{2}\tilde{\boldsymbol{e}} \end{bmatrix}, \tag{2}$$

where ${}_I\boldsymbol{v}_S$ is the translational velocity vector expressed in the frame I, and ${}_K\boldsymbol{\Omega}$ is the rotational velocity vector represented in the frame K.

3.2 Equations of motion

The time evolution of ${}_I\boldsymbol{v}_S$ is given by the balance of linear momentum:

$$m_{\mathrm{R}}\,{}_I\dot{\boldsymbol{v}}_S = {}_I\boldsymbol{F}_g + {}_I\boldsymbol{F}_c\,, \tag{3}$$

where m_{R} is the mass of the deadwood log. ${}_I\boldsymbol{F}_g$ is the gravitational force and ${}_I\boldsymbol{F}_c$ is the sum of all contact forces between the log and the terrain. The air resistance is neglected. Accordingly, the time evolution of ${}_K\boldsymbol{\Omega}$ obeys Euler's equation:

$${}_K\boldsymbol{\Theta}_S\,{}_K\dot{\boldsymbol{\Omega}} + {}_K\boldsymbol{\Omega} \times {}_K\boldsymbol{\Theta}_S\,{}_K\boldsymbol{\Omega} = {}_K\boldsymbol{M}_S\,, \tag{4}$$

where ${}_K\boldsymbol{\Theta}_S$ defines the inertia tensor for the log expressed in the frame K, and ${}_K\boldsymbol{M}_S$ is the net torque generated by contact forces acting on the boundary of the log. The geometry of the log is approximated by a point cloud defining a polytope. Each vertex may come in contact with the terrain, inducing a contact force at that vertex. The contact forces of all vertices are assembled in a tuple $\boldsymbol{\lambda}$. When the sliding log is not in contact with the terrain or surrounding trees, both ${}_I\boldsymbol{F}_c$ and ${}_K\boldsymbol{M}_S$ are zero. The equation of motion of the sliding deadwood can be summarised as:

$$\begin{cases} \mathbf{M}\dot{\boldsymbol{u}} - \boldsymbol{h}(\boldsymbol{q},\boldsymbol{u}) = \mathbf{W}(\boldsymbol{q})\,\boldsymbol{\lambda} \\ \mathbf{M} = \begin{bmatrix} m_{\mathrm{R}}\,\mathbf{I}_{3\times3} & \mathbf{0}_{3\times3} \\ \mathbf{0}_{3\times3} & {}_K\boldsymbol{\Theta}_S \end{bmatrix} \\ \boldsymbol{h}(\boldsymbol{q},\boldsymbol{u}) = \begin{pmatrix} {}_I\boldsymbol{F}_g, & -{}_K\boldsymbol{\Omega} \times {}_K\boldsymbol{\Theta}_S\,{}_K\boldsymbol{\Omega} \end{pmatrix}^T \end{cases} \tag{5}$$

Here, $\mathbf{M}$ is the diagonal mass matrix, $\boldsymbol{h}(\boldsymbol{q},\boldsymbol{u})$ contains the forces acting on the centre of mass (i.e. gravity and gyroscopic terms) and $\mathbf{W}(\boldsymbol{q})$ is the matrix of generalised force directions that transfers all the contact forces at the vertices on the log boundary to a corresponding force and torque at its centre of mass. Equation 5 together with contact laws is solved iteratively using Moreau's time-stepping scheme with a Gauss–Seidel iteration method (Studer, 2008).

3.3 Contact and impact laws

A contact between the log and the terrain is detected whenever at least one vertex of the log lies on or below the terrain surface (Leine et al., 2014). At every contact point, a local contact frame is defined with one normal and two tangential directions

https://doi.org/10.5194/egusphere-2026-130
Preprint. Discussion started: 24 March 2026
© Author(s) 2026. CC BY 4.0 License.

relative to the terrain surface. In the contact normal direction, the Signorini condition correlates the normal contact force λ_N and the normal gap g_N as follows:

$$0 \leq \lambda_N \perp g_N \geq 0. \tag{6}$$

In the contact tangential directions, the spatial Coulomb friction law is applied:

$$-\boldsymbol{\gamma}_T \in \begin{cases} \{\mathbf{0}\} & \text{if } \| \boldsymbol{\lambda}_T \| < \| \mu\lambda_N \|, \quad \text{sticking} \\ \mathbb{R}_0^+ \boldsymbol{\lambda}_T & \text{if } \| \boldsymbol{\lambda}_T \| = \| \mu\lambda_N \|, \quad \text{slipping} \end{cases} \tag{7}$$

where μ is the sliding friction coefficient. The contact force vectors $\boldsymbol{\lambda}_i = (\boldsymbol{\lambda}_{T,i}^T \, \lambda_{N,i})^T$ for 4 vertices are visualised in Fig. 2c.

Additionally, the hard contact approach requires an impact law, which, in combination with an impact equation, defines a mapping from pre- to post impact velocities. The impact law used for this model is based on the Newtonian impact law, which includes two cases (Leine and van de Wouw, 2008):

$$\gamma_N^+ + \varepsilon_N \gamma_N^- = 0 \ \wedge \ \Lambda_N > 0 \tag{8}$$

$$\gamma_N^+ + \varepsilon_N \gamma_N^- \geq 0 \ \wedge \ \Lambda_N = 0 \tag{9}$$

where γ_N^- and γ_N^+ are the normal pre- and post-impact velocity components, and ε_N is the normal restitution coefficient. The first case corresponds to an active impulsive contact force $\Lambda_N > 0$ whereas the second case describes a separation induced by impacts at other contact points. Consistent with rockfall modelling, we use a normal restitution coefficient of $\varepsilon_N = 0$, under the assumption that the restitution due to elastic deformations upon impact is negligible.

3.4 Interaction with standing trees and barriers

The contact detection between a sliding log and standing trees follows the algorithm by Lu et al. (2021), with its interaction also considered as hard contact. The standing trees are modelled as rigid, truncated cones with a DBH and h_S (see Fig. 2a). The energy dissipation caused by the uprooting and swaying of standing trees during an impact is not considered. Unlike the original tree model for rockfall applications, the standing trees do not have an energy threshold indicating a breaking failure during impact because of the assumption that the sliding deadwood will always break before the standing tree.

In addition, we include existing rockfall barriers in the model as thin, platy obstacles with the same impact behaviour as the standing trees. The barriers are rigid, have an infinite energy threshold and follow hard contact mechanics.

https://doi.org/10.5194/egusphere-2026-130
Preprint. Discussion started: 24 March 2026
© Author(s) 2026. CC BY 4.0 License.

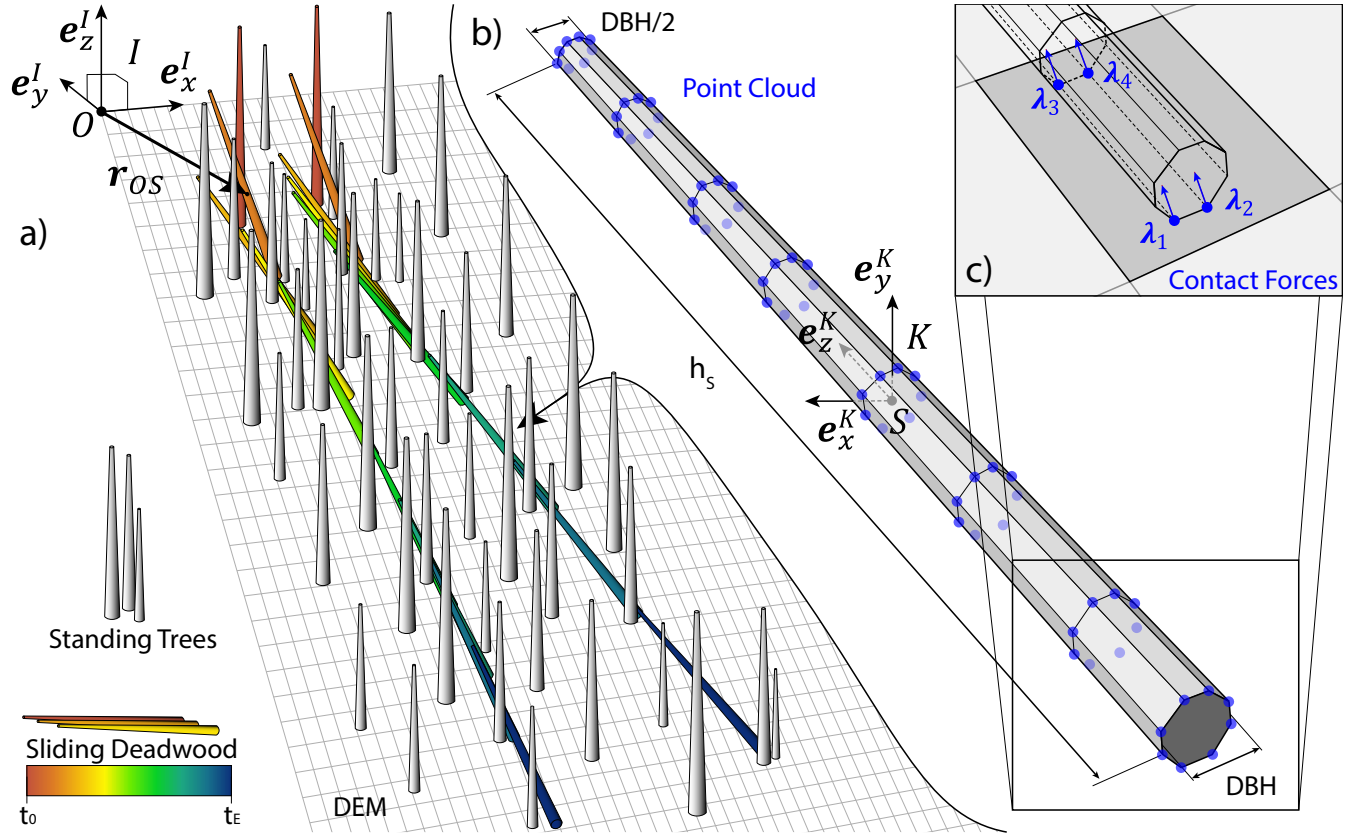

Figure 2. Simulation model of the sliding deadwood. a) DEM and standing trees are described in the inertial frame I. Two sliding deadwood logs are exemplary shown as a time series starting at the mobilisation time t_0 up to the deposition time t_E. b) Rigid, sliding deadwood with its geometry described as a point cloud in body-fixed frame K fixed at the centre of mass S. c) Contact between deadwood geometry and terrain with contact forces $\boldsymbol{\lambda}_i$ acting at vertex points of the point cloud.

4 Simulation setup

Due to the geometry of a log, the two main types of motion are either a sliding motion in the direction of the longitudinal axis, as shown in Fig. 2a or rolling around the longitudinal axis. Sliding requires either a steep slope or a low friction coefficient, while rolling is also possible on gentle slopes with high friction. However, in forested areas with standing trees, which is generally the case when considering the hazard of sliding deadwood, the standing trees will catch and block a rolling log. Therefore, sliding is the key process considered in this paper.

Fully deterministic models, such as the proposed one, require stochastic initial conditions to enable a statistical analysis of the results (Christen et al., 2012). In rockfall modelling, this is commonly achieved by varying the release locations or, if the rock shape is considered, by varying the initial orientation of the rock. For sliding deadwood, orientation variations mainly cause immediate interception by standing trees if logs are not aligned downslope. Therefore, the only way to introduce

https://doi.org/10.5194/egusphere-2026-130
Preprint. Discussion started: 24 March 2026
© Author(s) 2026. CC BY 4.0 License.

statistical variability is to use small spatial perturbations in the initial deadwood positions. To implement this, circular release polygons with a radius of 10 m are defined around the mapped release locations, within which the initial positions of the deadwood are randomly generated.

For the Klosters case study, the mobilised logs have a DBH of 75 cm and a length of $h_S = 30$ m, measured from the deposition of the first event (Fig. 1c). For Rothenbrunnen, the deadwood geometry is estimated from photographs of the deposition, yielding a DBH of 30 cm and a length of $h_S = 15$ m. For both case studies, the density of the released deadwood logs is assumed to be $\rho_S = 300$ kg m^{-3}. The initial orientation of the deadwood is always vertically upright. At the start of the simulation, the logs automatically align with the direction of steepest descent due to the low friction of the terrain (Fig. 2a).

It is important to note that, in reality, these initial conditions are considerably more complex. Mobilised snags may fall in any arbitrary direction, resulting in a variety of different initial momenta, whereas mobilised logs have no initial momentum at all, but still show a wide variety of initial orientations. In this paper, we generalise these initial conditions and focus on describing the sliding run-out behaviour given that the deadwood is mobilised.

The locations, DBH, and heights of the standing trees were derived using airborne laser scan (ALS) data from swisstopo (2020–2024), employing a single tree detection approach from Dalponte et al. (2015). Details on the determination of individual tree locations and heights are provided in Bast et al. (2025b). The DBH was then derived by applying an allometric power function to the detected tree heights, using parameter sets calibrated for the corresponding forest ecoregion and altitudinal vegetation zone (Bührle et al., 2025). The dataset containing the locations, DBH, and diameters of the individual trees used in this study is published in Bast et al. (2025a). In addition to the simulation with the actual forest, we also analyse a randomly generated forest with uniformly distributed tree positions based on the observed forest density and with DBH and tree heights sampled from normal distributions fitted to the values derived from the ALS in order to discuss the influence of forest structure. For Klosters, the ALS-based analysis yields a forest density of 300 stems ha^{-1}, with DBH normally distributed with a mean of $\mu_{\mathrm{DBH}} = 60.23$ cm and a standard deviation of $\sigma_{\mathrm{DBH}} = 18.64$ cm. For Rothenbrunnen, the corresponding forest density is 315 stems ha^{-1}, with DBH normally distributed with a mean of $\mu_{\mathrm{DBH}} = 44$ cm and a standard deviation of $\sigma_{\mathrm{DBH}} = 22$ cm. Finally, an additional scenario without forest is simulated to isolate and assess the protective effect of the forest itself.

These scenarios are compared using two main metrics. First, we quantify the probability p of reaching the infrastructure impacted in the observed event as

$$p = \frac{N_{\mathrm{reach}}}{N_{\mathrm{tot}}}, \tag{10}$$

where N_{reach} is the number of logs reaching the infrastructure and N_{tot} is the total number of released logs. Second, we compare the lateral spread $\Delta\theta$ of the individual events, which we define as the widest angle between any two deposition points when viewed from the release area

$$\Delta\theta = \max(\theta_i) - \min(\theta_i), \tag{11}$$

where θ_i is the azimuth angle of each deposition point (x_i, y_i) relative to the release point (x_0, y_0).

All simulations are performed on a 0.5 m DEM from 2023 (swisstopo, 2020–2024). The trajectories resulting from the 3D simulations are evaluated on the same 0.5 m grid as the DEM. We include the shape of the logs in this evaluation, which means

https://doi.org/10.5194/egusphere-2026-130
Preprint. Discussion started: 24 March 2026
© Author(s) 2026. CC BY 4.0 License.

that a trajectory is treated as the envelope of a moving polygon and not as a line without width. Consequently, at each time step, a simulated trajectory affects all cells that overlap any part of the deadwood geometry, not just its centre of mass. The model is implemented in the existing software RAMMS::Rockfall (Christen et al., 2014), which is used as a base framework for all simulations.

5 Simulation of case studies

5.1 Klosters, Graubünden (CH)

Given the initial conditions derived in Sect. 4, the only unknown model parameter left is the friction coefficient μ. The observed deposition pattern can be reproduced with a friction coefficient in the range of μ = 0.2–0.3. With higher friction, the road cannot be reached by the sliding deadwood. With lower friction, the logs do not stop on the road and continue sliding. The corresponding simulation results for a friction coefficient of μ = 0.25 are shown in Fig. 3a. We assume that all four events occurred with the same deadwood geometry and the same friction coefficient. The simulated deadwood logs show average velocities of 14 m s^{-1} with maximum velocities reaching 30 m s^{-1}. Out of the 20000 simulated logs, 1829 reach the national road, as determined by counting the number of trajectories intersecting the pink reference line shown in Fig. 3. This corresponds to a reach probability of 9.1 % according to Eq. 10. The lateral spread, calculated using Eq. 11, amounts to 40°, 60°, 60°, and 55°for events 1–4, respectively. Figure 3b presents the simulation results under the same conditions as Fig. 3a, but with all newly implemented protection measures in place. In the depicted section, these measures include two embankments and six rockfall barriers completed in 2024, which successfully reduce the probability of reaching the road to 0 %. Figure 3c shows the simulation results for the scenario with a randomly generated forest based on the forest density as well as the DBH and tree height distributions obtained from the ALS data. In this case, the probability of reaching the road is reduced to 7 % without a change in lateral spread compared to the case with the real forest structure. An exemplary magnified section below the first release polygon highlights the structural differences between the real forest (Fig. 3e) and the randomly generated forest (Fig. 3f). Lastly, Fig. 3d presents the scenario without any standing trees. In this case, the probability of reaching the road increases to 74.5 %, while the lateral spread for events 1–4 amounts to 23°, 31°, 25°, and 18°, respectively.

https://doi.org/10.5194/egusphere-2026-130
Preprint. Discussion started: 24 March 2026
© Author(s) 2026. CC BY 4.0 License.

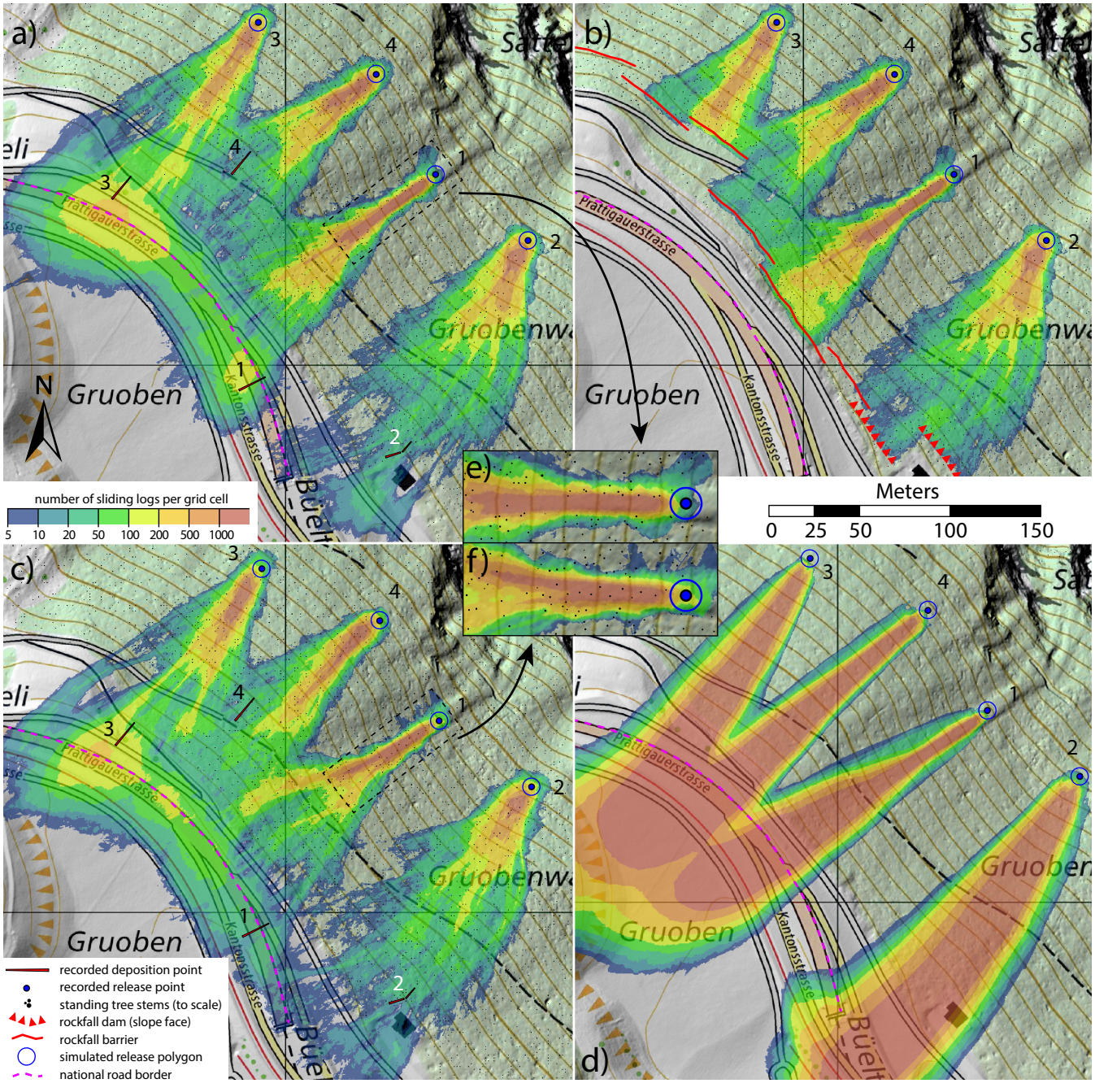

Figure 3. Reconstruction of the four events in Gruobenwald, Klosters (CH) with a friction coefficient of $\mu = 0.25$. The colours indicate how many of the 20000 released logs intersect their motion with each 0.5 × 0.5 m grid cell, revealing preferential sliding paths of the deadwood. a) Simulation without protection measures and ALS-based tree locations. b) Simulation with protection measures finished in 2024 and ALS-based tree locations. c) Simulation without protection measures and randomly generated forest. d) Simulation without protection measures and no forest. Two magnified sections below release 1 reveal the differences of the forest structure between ALS-based forest (e) and randomly generated forest (f). Map and hillshade from swisstopo (2020–2024).

https://doi.org/10.5194/egusphere-2026-130
Preprint. Discussion started: 24 March 2026
© Author(s) 2026. CC BY 4.0 License.

5.2 Rothenbrunnen, Graubünden (CH)

We can verify the hypothesis of the log jumping over the rockfall barrier by fitting a flight parabola between the presumed take-off and landing points. To obtain the 3D coordinates of the mapped points, they are projected onto a 0.5 m DEM. Since the log was sliding, the lift-off angle must have been equal to the local slope angle. We assume that only gravity acts on the log and that the longitudinal axis of the log is always parallel to the resulting velocity vector. The two projected points, together with the take-off angle, define a unique flight parabola. This parabola passes over the rockfall barrier (see Fig. 4c), which proves that such a jump is indeed possible. In addition, the uniquely defined take-off velocity of 24 m s^{-1} is within realistic bounds. In order to reach the required take-off velocity to jump over the barrier with the proposed 3D model, a friction coefficient of $\mu < 0.3$ is required, which corresponds to the same maximum allowable friction to reconstruct the events in Klosters. Contrary to the Klosters case, however, it is not possible to derive a minimum required friction, as the log was not stopped gradually by friction between log and terrain but abruptly by a guardrail. The 3D simulations confirm that it is possible that a mobilised tree jumps over the rockfall barrier. According to the simulation shown in Fig. 4a, 1442 of the initially 20000 released logs reached the southernmost barrier of which 1264 were stopped and 178 jumped over. This results in a reach probability of the observed event of 0.9 % according to Eq. 10. This probability is small but reasonable given the fact that such an event has never been recorded despite the high number of mobilisations observed. A plausible 3D trajectory of the observed event can be found in Appendix A, Fig. B1. Additionally, we can demonstrate the efficiency of the existing rockfall barriers by removing all protection measures in a simulation (see Fig. 4b). In this case, 4658 logs (23.3 %) reach the road.

https://doi.org/10.5194/egusphere-2026-130
Preprint. Discussion started: 24 March 2026
© Author(s) 2026. CC BY 4.0 License.

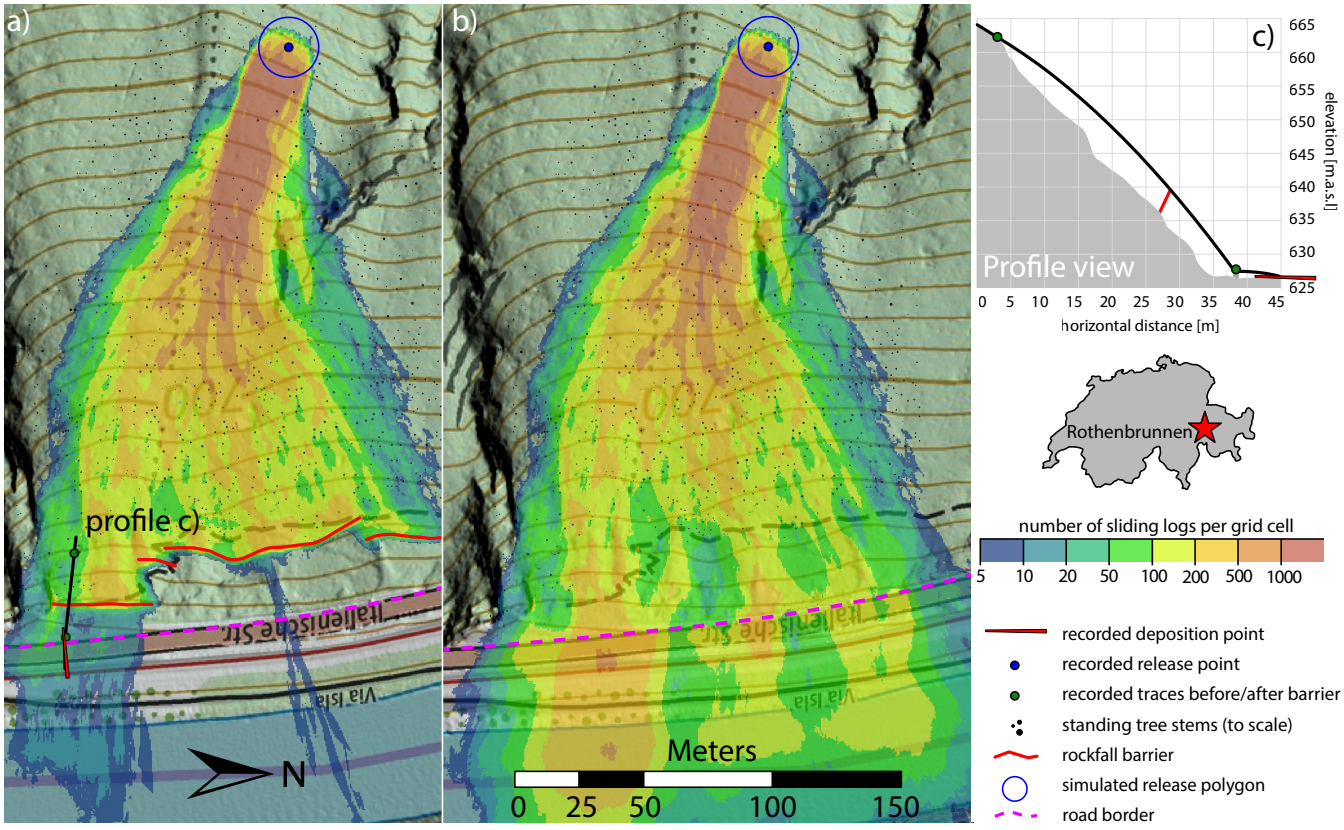

Figure 4. Reconstruction of the 2022 event in Plattawald, Rothenbrunnen (CH). All simulations were done with 20000 randomly distributed upright logs within the release polygon and a friction coefficient of $\mu = 0.25$. The colours indicate how many of the 20000 released logs intersect their motion with each 0.5×0.5 m grid cell, revealing preferential sliding paths of the deadwood. a) Simulation with ALS-based tree locations and rockfall barriers. b) Simulation with ALS-based tree locations without barriers. c) Profile view in the vicinity of the presumably overjumped rockfall barrier with fitted flight parabola. Map and hillshade from swisstopo (2020–2024).

6 Discussion

6.1 Factors promoting deadwood sliding hazards

The documented cases of sliding deadwood highlight three key factors contributing to the risk of sliding deadwood impacting infrastructure below: (1) low friction; (2) steep slopes; and (3) early-stage wood decomposition:

Low friction either occurred due to terrain conditions (e.g. wet soil, snow, foliage cover), the condition of the deadwood (wet log without bark and branches) or a combination of both. Physically, a sliding movement is possible for a friction coefficient of $\mu < \tan\psi$, where ψ is the slope inclination. The proposed model can reconstruct both case studies with a friction coefficient in the range of $\mu = 0.2$–0.3, which therefore describes the typical contact friction between wet terrain and a wet log without

https://doi.org/10.5194/egusphere-2026-130
Preprint. Discussion started: 24 March 2026
© Author(s) 2026. CC BY 4.0 License.

bark and branches. A friction coefficient of $\mu = 0.3$ means that under these conditions, a mobilisation is theoretically possible at slope angles $\psi > 18°$. For a slope angle of 30°, a mobilisation is possible for $\mu < 0.58$.

All events occurred in very steep forests with slope angles $\psi \geq 35°$. While this is directly linked to the first criterion, slope angle warrants a separate discussion. In a typical multibody simulation of relatively smooth contacting bodies, the Coulomb friction model is used to account for sliding resistance due to various abrasive processes which take place on a microscopic scale. These frictional processes are highly complex, depend heavily on the microscopic roughness, and are quite bluntly described by the Coulomb friction model through a single parameter, being the friction coefficient μ. In the modelling of sliding deadwood (and also rockfall), the macroscopic roughness is modelled through the chosen resolution of the DEM. The roughness effects which fall below the resolution of the DEM is to be accounted for by the Coulomb friction model. This macroscopic roughness of the DEM implies that very steep forests with $\psi \geq 35°$are a requirement for deadwood mobilisation even though the calibrated $\mu = 0.2$–0.3 suggests a minimum required slope angle of 12–18°. This also implies that the calibrated μ is only valid for the DEM resolution of 0.5 m and should be increased accordingly when working with lower resolution DEMs.

All of the recorded events occurred with fresh deadwood with early-stage wood decomposition. More specifically, the decay was advanced to the point where the trees have lost their branches and bark to reduce sliding friction. At the same time, the trees still showed sufficient structural strength so that they did not break on impacts while sliding. According to the decay stage classification by Maser and Trappe (1984), this deadwood state corresponds to a late stage II or early stage III. In this critical decay stage, a pocket knife can penetrate the wood only in the direction of the fibres but not in perpendicular direction (Lachat et al., 2014). For a case study on a spruce forest with bark beetle infestation, this critical decay stage was reached 2–5 years after death (Ammann, 2006). The critical time period, however, heavily depends on the tree species. Herrmann et al. (2015) showed that beech has significantly higher decay rates than spruce or pine. Additional influencing factors are the stem diameter (Holeksa et al., 2008), temperature, humidity and contact to the ground (Petrillo et al., 2016). This critical decay stage also explains why the majority of deadwood mobilised in the presented events were snags triggered by an active mobilisation mechanism (e.g. windthrow, rockfall, snow weight or logging). Only in the Rothenbrunnen case study, it is unclear from the documentation whether the deadwood was initially standing or lying. Active mobilisation is important especially for snags because if a snag falls purely due to decay without any additional loads, it is very likely that it will immediately break apart on impact and therefore cannot slide over long distances. Lying deadwood may also be mobilised at sufficient structural strength (e.g. by rockfall or erosion). However, since it has already withstood a major mobilisation event when the respective tree or snag initially fell, it must be held back by significant resistance, such as terrain roughness, blocking trees, or other deadwood, making remobilisation inherently more difficult. In fact, lying deadwood may even help reduce the hazard potential of sliding deadwood, as it acts as a natural barrier, blocking or slowing down mobilised logs, provided it is itself firmly locked in place.

While all three factors are prerequisites for risks from sliding logs, local natural conditions can vary significantly. The first case study shows a typical critical combination of conditions which fulfil all the criteria for sliding deadwood, where a steep forest with previous bark beetle infestation led to several snags without bark and branches (reduced friction) and is later hit by

https://doi.org/10.5194/egusphere-2026-130
Preprint. Discussion started: 24 March 2026
© Author(s) 2026. CC BY 4.0 License.

a storm (reduced friction due to rain, active mobilisation mechanism due to wind). The second case study shows that wet snow can also be critical, as it causes mechanical stress on trees and at the same time reduces friction.

6.2 The role of forest structure

Standing trees influence sliding deadwood in two distinct ways, each affecting the hazard differently. On the one hand, trees act as effective physical barriers that can block or arrest sliding logs, particularly when the longitudinal axis of a log is misaligned with its velocity vector. This protective effect is clearly reflected in the simulation results. In the Klosters case study, the probability of sliding logs reaching the road increases from 9.1 % for the simulation with standing trees to 74.5 % when the forest is removed. In the Rothenbrunnen case study, the reach probability increases from 23.3 % with standing trees to 100 % without forest (see Appendix A, Fig. A1). These results demonstrate that the forest itself represents a highly effective protective measure against hazards caused by its own mobilised deadwood.

On the other hand, standing trees can deflect sliding logs, increasing lateral spread. Due to their elongated shape, logs can traverse slopes over long distances and often deviate substantially from the steepest descent direction. Once a log enters a traverse motion, realignment with the fall line becomes unlikely, as its length and repeated interactions with standing trees hinder rotational adjustment. In the Klosters case study, the simulated lateral spread amounts to 40°, 60°, 60°, and 55°for events 1–4. When the simulations are repeated without forest, the lateral spread decreases to 23°, 31°, 25°, and 18°, respectively. For the Rothenbrunnen case study, the same comparison shows a reduction in lateral spread from 49°to 18°(see Appendix A, Fig. A1).

A key observation from the events in Klosters is that the deadwood tends to slide further when the simulation is run with tree locations and DBH from the ALS instead of a randomly generated forest with the same tree density and DBH distribution. For the simulation shown in Fig. 3a, the probability of reaching the road decreases from 9.1 % with the ALS tree data to 7.0 % with the randomly generated forest. The reason for this decline is that the preferred path of the sliding deadwood is determined by the micro-topography (e.g. sliding in ditches, valleys, gullies). In a randomly generated forest, these preferred paths can be blocked by standing trees. In reality, however, these gullies are often treeless or less densely forested due to rockfall, avalanche dynamics, and other channel processes, as well as unfavourable site conditions related to persistent snow cover and competition from herbaceous vegetation (Barbeito et al., 2012). The comparison between Figs. 3e and 3f highlights the importance of using ALS–derived tree locations: while the preferential sliding path is largely vegetation-free in the real forest, it is obstructed in the randomly generated forest, leading to an underestimation of the hazard potential.

In contrast, the Rothenbrunnen case study shows a smaller difference between simulations using ALS tree data and a randomly generated forest. For the simulation shown in Fig. 4b, the probability of reaching the road even increases slightly from 23.3 % with the ALS tree data to 23.8 % with the randomly generated forest (Appendix A, Fig. A1). This negligible difference can be explained in this case by the fact that there are no clear preferential sliding paths in gullies that could be blocked by randomly generated trees. This suggests that in non-channelised terrain, precise tree locations are less important, as there are no distinct preferential sliding paths that could be blocked by randomly placed trees. Nonetheless, individual tree data remains valuable for accurately determining forest stem density.

https://doi.org/10.5194/egusphere-2026-130
Preprint. Discussion started: 24 March 2026
© Author(s) 2026. CC BY 4.0 License.

6.3 Sliding deadwood in the context of other natural hazards

Steep mountain forests, where sliding deadwood is possible, often serve as protection against natural hazards. These areas, prone to sliding trees, are thus typically also exposed to rockfalls, avalanches or landslides. Compared to rocks in rockfall hazard scenarios, deadwood logs have a less favourable shape, lower strength and density than rocks, generally resulting in reduced velocities, kinetic energies and run-out distances. This may suggest that, in most cases, the danger from sliding deadwood plays a relatively minor role in the planning of protective measures such as barriers or embankments. However, there are some conditions where a hazard analysis of sliding deadwood should be considered:

1. According to our work, the risks posed by sliding deadwood in protection forests and natural hazard management are relevant only in specific situations. In most forested areas with relatively gentle slopes ($< \sim 35°$) and high roughness, deadwood can mitigate rockfall and avalanche risks and support sustainable forest regeneration (Ringenbach et al., 2022b; Caduff et al., 2022). However, along steep gullies with low surface roughness, it may be necessary to assess whether removing dying or dead trees or actively cutting and securing them across the slope is appropriate to reduce overall gravitational hazard risks.

2. Simulations with the proposed model show that sliding deadwood can deviate significantly from the steepest descent suggesting a greater lateral spread than rockfalls. When the simulation shown in Fig. 4b is performed with rocks and ground parameters calibrated for a spruce/beech forest (Ringenbach et al., 2023), the resulting lateral spread decreases from 49°for the deadwood simulation to 40°for a 1 m^3 platy rock and 35°for a 1 m^3 cubic rock. This means that deadwood may reach unprotected infrastructure by traversing a slope.

3. Despite only few documented cases, the risk to roads, buildings, and infrastructure from sliding deadwood is expected to increase with the rising frequency and intensity of natural disturbances (Seidl et al., 2017)

4. Under the specific conditions which potentially enable deadwood to slide, protective structures must be designed to stop slender objects such as sliding deadwood. This is particularly critical for ring nets with large ring diameters. Depending on the deposition configuration of a log stopped by a rockfall barrier, not clearing the deadwood from the net can lead to a reduction in the braking distance and thus to a lower energy absorption capacity for future rockfall events.

In both case studies, sliding deadwood reached infrastructure despite protective measures. In Klosters, this was due to outdated protective structures (wooden palisades) or a lack of protective measures in some places. In Rothenbrunnen, deadwood was able to jump over a barrier positioned below a terrace. When considering implications for natural hazard management, it is important to note that: 1) a rockfall in both cases could have caused similar or greater damage, and 2) perfect protection is hardly ever guaranteed due to construction constraints like barrier height or length. Nevertheless, the comparisons between scenarios with and without protection, as shown in Figs. 3 and 4, highlight the overall efficiency of the current measures. Although events involving sliding deadwood highlight significant hazards and, depending on topography, can expand the lateral extent of risk zones, the need for additional structural measures must be carefully evaluated.

https://doi.org/10.5194/egusphere-2026-130
Preprint. Discussion started: 24 March 2026
© Author(s) 2026. CC BY 4.0 License.

6.4 Implications for forest management

The decision to leave deadwood in the forest depends on the local natural conditions, the relative importance assigned to biodiversity and various forest functions and potential effects on subsequent disturbances (Costa et al., 2021; Leverkus et al., 2021). Regarding the deadwood's role in natural hazard protection, its changing effects over time are particularly significant (Caduff et al., 2022). Ammann (2006) showed from large-scale laboratory tests that the fracture impact energy of a log is reduced by up to 89 % in 8-10 year old deadwood with rot fungus compared to fresh deadwood. As the structural strength is also important for the protective effect of deadwood, the age of the deadwood is linked to competing positive and negative effects, emphasising the need for an integral view on deadwood from a forest management perspective. Deadwood in its earliest stages shows high structural strength and thus a high protective effect against rockfall and avalanches, but temporarily offers often suitable habitat for bark beetles in spruce-dominated forests (Wermelinger, 2004). In a later decay stage (2–5 years after death for spruce), structural strength and protective effect still remains intact, while at the same time, the hazard of sliding logs increases. In the advanced decay stage (5+ years after death in spruce), the risk of sliding deadwood decreases, but so does its protective effect. Conversely, the ecological value of deadwood continues to increase, particularly as a habitat and, typically after more than 20 years (Piazza et al., 2024), as a substrate for seedling establishment, thereby promoting forest regeneration.

This trade-off also applies spatially. Although deadwood logs in gullies have a higher sliding hazard potential, they also offer increased protection against other natural hazards. For rockfall, these gullies are preferred rolling paths and therefore an optimal location for a natural barrier. In the case of avalanches, deadwood logs stabilise the snow cover in these less vegetated areas (Schönenberger et al., 2005; Baggio et al., 2022). Our study sheds light on an often overlooked but, in specific situations, important effect of deadwood, helping to decide where and when retaining deadwood is overall beneficial, and where alternative management approaches, such as removal or controlled relocation and stabilisation, may be more appropriate.

In addition, the strong protective effect of standing trees against sliding deadwood implies a spatial differentiation of hazard within forested slopes. Logs mobilised high on a forested slope still traverse a long forested runout path and therefore have multiple opportunities to be intercepted by standing trees. In contrast, logs mobilised in the lower parts of the forest encounter little or no forest remaining downslope, which substantially increases the likelihood of reaching exposed infrastructure. This suggests that snags and deadwood located in lower forest sections that are still sufficiently steep may require particular attention in hazard assessments, and that interventions such as felling should be carried out with caution in these areas.

6.5 Model limitations

Despite the high level of process detail incorporated through a physically based modelling framework coupled with high-resolution ALS tree data, several limitations remain. Firstly, sliding deadwood is represented as rigid bodies that do not fracture upon impact. While this neglects potential breakage at advanced decay stages, it is fully consistent with the objective of this study. The purpose of the model is not to simulate all possible deadwood conditions, but to quantify runout, lateral spread, and hazard potential under those specific conditions that make sliding deadwood hazardous. As shown in Sect. 6.1, these conditions correspond to a narrow decay-stage window in which sufficient residual structural strength is still present to allow

https://doi.org/10.5194/egusphere-2026-130
Preprint. Discussion started: 24 March 2026
© Author(s) 2026. CC BY 4.0 License.

long-distance transport without immediate fragmentation. The model is therefore explicitly conditioned on a prior assessment of decay stage: only logs that fall within this critical structural state are considered potential hazards and simulated. Under this premise, assuming non-breaking rigid logs is appropriate. At the same time, this assumption yields conservative, worst-case estimates of runout and impact probability, since even structurally strong logs may still break depending on impact velocity and configuration. Logs in more advanced decay stages are expected to fragment early and thus pose a substantially lower hazard, but are outside the intended scope of the present model.

The initial conditions of the simulations introduce an additional limitation. Logs are released in a simplified, upright configuration and randomly positioned within the specified release area, without explicitly modelling the true mechanical triggering process or the transition from toppling to sliding. This idealisation may influence the very early phase of motion, particularly the initial orientation of the log. However, this is fully consistent with the intended application of the model: the mobilisation potential of deadwood is first assessed based on decay stage, terrain inclination, and local site conditions. The simulation tool is then applied under the explicit condition that mobilisation is already deemed possible, in order to quantify runout and lateral spread. This separation between mobilisation assessment and runout modelling follows standard hazard-modelling practice.

Additional simplifications include the rigid and indestructible representation of standing trees, which neglects energy dissipation due to tree swaying, uprooting, breaking or soil–root interactions during impacts. This again leads to slightly conservative estimates of runout and lateral spread. Furthermore, friction is represented by a single effective Coulomb coefficient that implicitly incorporates microscopic surface roughness effects. As discussed in Sect. 6.1, this parameter is resolution-dependent and valid only for the DEM resolution of 0.5 used in this study. Despite these limitations, the model reliably reproduces the observed deposition patterns of documented events and fulfils its intended purpose: providing conservative, physically consistent estimates of runout and lateral spread conditional on a prior mobilisation assessment.

6.6 Model usage and transferability

The sliding deadwood model can be applied directly by any user with access to RAMMS::Rockfall, without requiring code-level modifications or a special software version. A simulation is set up following the standard rockfall workflow, including the definition of release areas and forest. To suppress scarring effects, the ground mechanical properties are set to a high M_E (e.g. M_E = 1000 MPa) and a zero drag coefficient (C_D = 0). The friction coefficient of the slope is then defined by manually editing the input XML file and setting $\mu_{\min} = \mu_{\max}$ equal to the desired effective Coulomb friction coefficient.

The geometry of the sliding log is generated externally, for example using a Python script, based on a chosen DBH and log length, which can then be imported as a custom rock shape in RAMMS.

The presented sliding deadwood model is physically tailored to a rigid-body solver that explicitly resolves frictional contact and interactions with individual trees. In principle, it can only be transferred to numerical frameworks that fulfil three essential requirements:

1. Representation of the moving object as an extended rigid body rather than a lumped mass or spherical particle

2. Explicit resolution of contact forces and Coulomb friction in 3D, allowing for physically consistent sliding motion

https://doi.org/10.5194/egusphere-2026-130
Preprint. Discussion started: 24 March 2026
© Author(s) 2026. CC BY 4.0 License.

3. Discrete representation of individual standing trees as geometric obstacles

If sliding deadwood were approximated as a lumped mass or spherical particle, as is done in many existing models, the simulation would lose all information on object orientation, contact length, and rotational resistance. Characteristic deadwood behaviour such as long-distance basal sliding, lateral deflection due to asymmetric contact, and alignment of the stem with the local slope would therefore be physically misrepresented. This would systematically bias runout distances and lateral spread. Models allowing non-spherical, simplified rock geometries (Dorren, 2024; Agliardi and Crosta, 2003; Andrew et al., 2012; Noël et al., 2021) could, in principle, be adapted to represent logs as elongated ellipsoids or cylinders, but they lack a rigid-body physics engine to resolve the continuous orientation and alignment of the log. In addition, they rely on restitution-coefficient-based impact behaviour, which cannot represent the low-impact, friction-controlled dynamics of sliding logs.

Rockfall models with a physical rigid-body framework, such as the model by Yan et al. (2020) or Rocfall3 (Rocscience Inc., 2024), could in principle reproduce the sliding behaviour of the logs if the log geometry were explicitly incorporated into the model. However, these models do not represent forests with distinct individual trees. In this case, the strong directional control exerted by individual standing trees is lost. The simulations in this study show that single tree impacts dominate lateral deflection, trajectory splitting, and final deposition patterns of sliding logs. Without explicit trees, both lateral spread and reach probabilities would be systematically biased.

Beyond rockfall-specific software, general-purpose rigid-body and nonsmooth contact solvers such as Siconos (Acary et al., 2019) or physics engines such as pyBullet (Coumans and Bai, 2016–2020) would, in principle, satisfy the mechanical requirements for sliding deadwood. However, applying these tools to natural hazard assessment would require rebuilding all essential components for terrain handling, forest representation, stochastic release generation, and hazard-relevant post-processing, making them impractical for immediate operational use.

7 Conclusions

The findings from our case studies highlight the key factors influencing the hazard of sliding deadwood: low friction, very steep slopes, and early-stage wood decomposition. Our model successfully reconstructs observed events with a friction coefficient in the range of μ = 0.2–0.3 on a DEM resolution of 0.5 m, reinforcing the importance of surface conditions and terrain roughness in deadwood mobilisation. While very steep slopes ($> \sim 35°$) are a prerequisite for sliding, local surface roughness significantly impacts the threshold at which movement occurs. The study further emphasises that deadwood in a critical decay stage (2–5 years after death for spruce) exhibits reduced friction while still maintaining sufficient structural integrity to slide long distances without breaking upon impacts. In all presented cases, these conditions were a result of an active triggering mechanism, such as storms, snow loads, rockfalls or logging. The observed events indicate that snags pose the greatest hazard due to their initial momentum when falling. Lying deadwood may also be mobilised in less frequented cases, but can also serve as a natural barrier, blocking or slowing down sliding deadwood. These findings underline that sliding deadwood represents a relevant hazard only under a narrow combination of conditions and does not constitute a widespread or persistent risk in most forested slopes.

https://doi.org/10.5194/egusphere-2026-130
Preprint. Discussion started: 24 March 2026
© Author(s) 2026. CC BY 4.0 License.

Our results demonstrate that forest structure plays a crucial role in sliding deadwood dynamics, affecting both run-out distances and the lateral spread of logs. The presence of standing trees can either block movement or deflect logs. The simulations clearly show that standing trees provide an effective first line of protection against hazards caused by their own mobilised deadwood. Removing forest cover leads to a drastic increase in reach probabilities, demonstrating that intact forests can substantially limit runout and reduce the likelihood of sliding deadwood reaching exposed infrastructure. Simulations indicate that natural tree distributions, particularly less densely vegetated gullies, facilitate preferred paths for sliding logs, a factor that should be considered in hazard assessments. High-resolution ALS data helps to identify critical gullies and channels in a forest (which is also extremely important for other natural hazard processes) and to correctly determine the spatial distribution of single trees in these sensitive areas. As a result, measures in protection forests can be better prioritised, including the early removal of snags or actively cutting and securing them across the slope.

Managing deadwood in mountain forests remains challenging. Areas most susceptible to deadwood mobilisation often overlap with zones crucial for mitigating other natural hazards. Likewise, the decay stages at which snags and logs are most prone to move are the very stages in which their structural strength still contributes to protection. Although the framework presented here cannot eliminate these trade-offs, it supports the identification of the most critical locations and deadwood conditions. By applying targeted measures in these critical areas on deadwood in critical conditions, the hazard of sliding deadwood can be minimised, while the protective and ecological benefits of deadwood in mountain forests are largely retained.

Code and data availability. The point cloud files of the deadwood logs used in the simulations, as well as the Python code used to generate these geometries, will be published in an EnviDat repository with associated DOI upon acceptance of the manuscript.

Appendix A: Rothenbrunnen supplementary simulations

This appendix presents additional simulation results for the Rothenbrunnen case study, analogous to the Klosters case study (see Sect. 5.1), including scenarios with a randomly generated forest and without forest. All simulations were performed using the same initial conditions, consisting of 20000 upright logs randomly distributed within the release polygon and the same friction coefficient of $\mu = 0.25$.

Figure A1a shows the scenario without any standing trees, resulting in a probability of reaching the road, according to Eq. 10, of 100 % and a lateral spread of 18°. Figure A1b presents the simulation results for the scenario with a randomly generated forest based on the forest density as well as the DBH and tree height distributions derived from the ALS. In this case, the probability of reaching the road is 23.8 %, while the lateral spread remains identical to that of the ALS-derived forest scenario at 50°.

https://doi.org/10.5194/egusphere-2026-130
Preprint. Discussion started: 24 March 2026
© Author(s) 2026. CC BY 4.0 License.

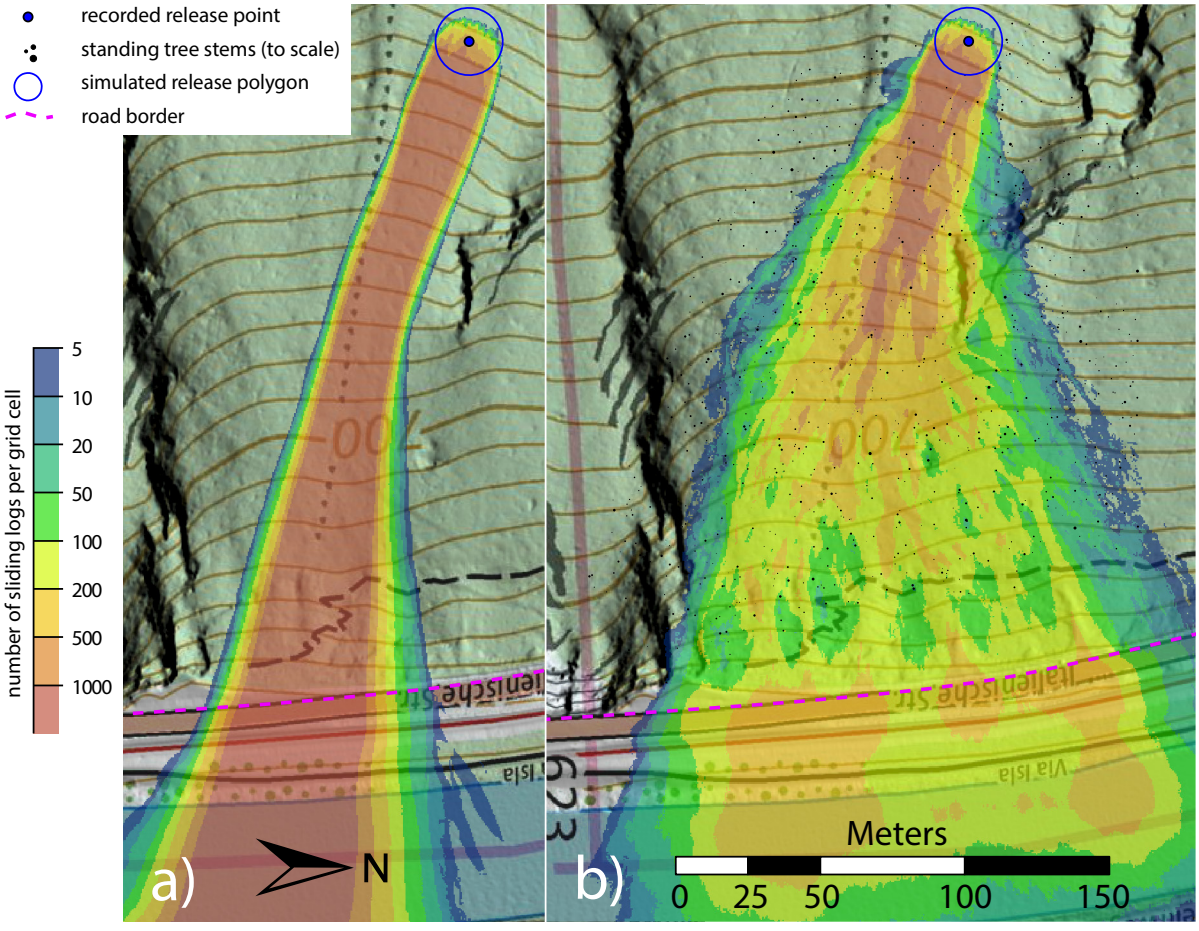

Figure A1. Additional simulations based on the 2022 event in Plattawald, Rothenbrunnen (CH). All simulations were performed with 20000 randomly distributed upright logs within the release polygon and a friction coefficient of $\mu = 0.25$. The colours indicate the number of logs intersecting each 0.5 m $\times$ 0.5 m grid cell, highlighting preferential sliding paths of the deadwood. a) Simulation without forest. b) Simulation with a randomly generated forest. Map and hillshade from swisstopo (2020–2024).

Figure B1 illustrates a representative trajectory from the three-dimensional simulation that plausibly reproduces the documented event. The simulated log lifts off near the location of the last recorded trace before the barrier due to a local plateau at a velocity of 27.8 m s^{-1} (compared to the reconstructed value of approximately 24 m s^{-1}; see Sect. 5.2), and jumps over the barrier. The simulated trajectory results in a maximum jump height of 9.9 m, defined as the vertical distance between the log's centre of mass and the terrain, before the log lands on the road close to the first recorded trace downstream of the barrier.

https://doi.org/10.5194/egusphere-2026-130
Preprint. Discussion started: 24 March 2026
© Author(s) 2026. CC BY 4.0 License.

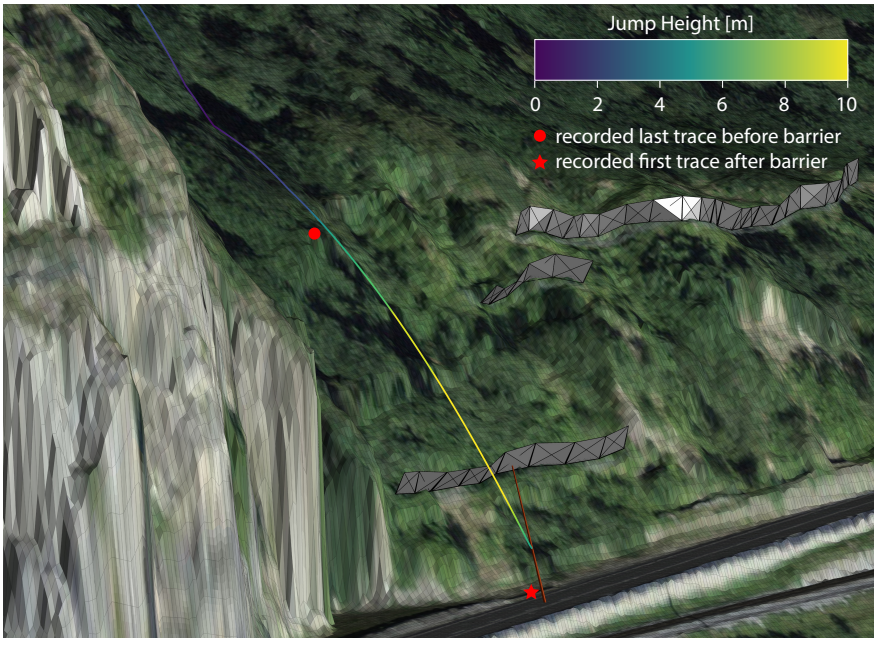

Figure B1. Three-dimensional simulation of a representative sliding deadwood trajectory at the Rothenbrunnen site. The figure shows the simulated log position at the time step when the log first touches the terrain after the jump over the barrier. The jump is initiated by a local plateau upslope of the barrier, leading to a maximum jump height of 9.9 m (measured as the vertical distance between the log centre of mass and the terrain) and a velocity of 27.8 m s^{-1} at take-off. Background orthophoto from swisstopo (2020–2024).

Author contributions. JB conceptualised the idea and formulated the aims and methodology of the study. JB and RL developed the model framework. JB and PB researched the case studies. AR and LB pre-processed the ALS data for the simulations. JB performed the simulations and post-processed the data. JB led the interpretation of the results and the development of the discussion, with substantial contributions from PB and LB through targeted literature research and scientific guidance. JB prepared the manuscript with contributions from all co-authors.

Competing interests. The authors declare that they have no conflict of interest.

Acknowledgements. The authors would like to thank Flurin Wehrli from the Madrisa forestry operation and the Office for Forests and Natural Hazards of the Canton of Graubünden (AWN GR) for providing the necessary documentation of the sliding deadwood events. Furthermore, the authors would like to thank Dr. Perry Bartelt and Marc Christen from RAMMS AG for providing the RAMMS::Rockfall software and their support in adapting the modelling framework. During the preparation of this work, the authors used ChatGPT 5 to improve the readability of some sentences. After using this tool/service, the authors reviewed and edited the content as needed and take full responsibility for the content of the publication.

https://doi.org/10.5194/egusphere-2026-130
Preprint. Discussion started: 24 March 2026
© Author(s) 2026. CC BY 4.0 License.

References

Abegg, M., Ahles, P., Allgaier Leuch, B., Cioldi, F., Didion, M., Düggelin, C., Fischer, C., Herold, A., Meile, R., Rohner, B., Rösler, E., Speich, S., Temperli, C., and Traub, B.: Swiss national forest inventory - Result table No. 2314378, 2023a.

Abegg, M., Ahles, P., Allgaier Leuch, B., Cioldi, F., Didion, M., Düggelin, C., Fischer, C., Herold, A., Meile, R., Rohner, B., Rösler, E., Speich, S., Temperli, C., and Traub, B.: Swiss national forest inventory - Result table No. 1382008, https://doi.org/10.21258/1815384, 2023b.

Acary, V. and Brogliato, B.: Numerical methods for nonsmooth dynamical systems, Lecture notes in applied and computational mechanics, Springer, 2008 edn., https://doi.org/10.1007/978-3-540-75392-6, 2008.

Acary, V., Bonnefon, O., Brémond, M., Huber, O., Pérignon, F., and Sinclair, S.: An introduction to Siconos, Technical Report RT-0340, INRIA, https://inria.hal.science/inria-00162911, 2019.

Agliardi, F. and Crosta, G.: High resolution three-dimensional numerical modelling of rockfalls, International Journal of Rock Mechanics and Mining Sciences, 40, 455–471, https://doi.org/10.1016/S1365-1609(03)00021-2, 2003.

Ammann, M.: Schutzwirkung abgestorbener Bäume gegen Naturgefahren, Ph.D. thesis, ETH Zurich, https://doi.org/10.3929/ETHZ-A-005268444, 2006.

Andrew, R., Hume, H., Bartingale, R., Rock, A., and Zhang, R.: CRSP-3D user's manual—Colorado Rockfall Simulation Program, https://coloradogeologicalsurvey.org/publications/colorado-rockfall-simulation-program/, 2012.

Baggio, T., Brožová, N., Bast, A., Bebi, P., and D'Agostino, V.: Novel indices for snow avalanche protection assessment and monitoring of wind-disturbed forests, Ecological Engineering, 181, 106 677, https://doi.org/10.1016/j.ecoleng.2022.106677, 2022.

Barbeito, I., Dawes, M. A., Rixen, C., Senn, J., and Bebi, P.: Factors driving mortality and growth at treeline: a 30-year experiment of 92 000 conifers, Ecology, 93, 389–401, https://doi.org/10.1890/11-0384.1, 2012.

Bast, A., Hobi, M., Ginzler, C., Piermattei, L., Fischer, C., Nikolova, P. S., Bührle, L., and Kalt, T.: Individual Detected Trees, https://doi.org/10.16904/envidat.696, 2025a.

Bast, A., Hobi, M. L., Ginzler, C., Piermattei, L., Fischer, C., Nikolova, P. S., Bührle, L. J., Kalt, T., and Graf, F.: An approach to detect and map forest canopy layers in Swiss mountain forests using nationwide airborne laser scanning data, International Journal of Applied Earth Observation and Geoinformation, 145, 104 986, https://doi.org/10.1016/j.jag.2025.104986, 2025b.

Bebi, P., Putallaz, J.-M., Fankhauser, M., Schmid, U., Schwitter, R., and Gerber, W.: Die Schutzfunktion in Windwurfflächen, Schweizerische Zeitschrift fur Forstwesen, 166, 168–176, https://doi.org/10.3188/szf.2015.0168, 2015.

Bourrier, F., Dorren, L., and Berger, F.: Full scale field tests on rockfall impacting trees felled transverse to the slope, in: 12th Congress INTERPRAEVENT 2012, p. 8, Grenoble, France, https://hal.inrae.fr/hal-02597700, 2012.

Bührle, L. J., Kalt, T., Bebi, P., Teich, M., Hobi, M. L., Bast, A., Schrott, R., Helzel, K., Temperli, C., Bont, L. G., Blattert, C., Schweier, J., and Bottero, A.: Regional disturbance predisposition assessment to support management in mountain spruce forests, https://doi.org/10.2139/ssrn.5852106, manuscript under review, 2025.

Caduff, M. E., Brožová, N., Kupferschmid, A. D., Krumm, F., and Bebi, P.: How large-scale bark beetle infestations influence the protective effects of forest stands against avalanches: A case study in the Swiss Alps, Forest Ecology and Management, 514, 120 201, https://doi.org/10.1016/j.foreco.2022.120201, 2022.

Christen, M., Bühler, Y., Bartelt, P., Leine, R., Glover, J., Schweizer, A., and Volkwein, A.: Integral hazard management using a unified software environment. Numerical simulation tool "RAMMS" for gravitational natural hazards, in: 12th Congress INTERPRAEVENT

https://doi.org/10.5194/egusphere-2026-130
Preprint. Discussion started: 24 March 2026
© Author(s) 2026. CC BY 4.0 License.

2012. Grenoble, France. Conference proceedings "Protection of living space from natural hazards", edited by Koboltschnig, G., Hübl, J., and Braun, J., pp. 77–86, 2012.

Christen, M., Schweizer, A., Leine, R., Caviezel, A., and Bartelt, P.: RAMMS::Rockfall, https://ramms.ch/ramms-rockfall/, 2014.

Costa, M., Marchi, N., Bettella, F., Bolzon, P., Berger, F., and Lingua, E.: Biological legacies and rockfall: The protective effect of a windthrown forest, Forests, 12, https://doi.org/10.3390/f12091141, 2021.

Coumans, E. and Bai, Y.: PyBullet, a Python module for physics simulation for games, robotics and machine learning, http://pybullet.org, 2016–2020.

Dalponte, M., Reyes, F., Kandare, K., and Gianelle, D.: Delineation of individual tree crowns from ALS and hyperspectral data: a comparison among four methods, European Journal of Remote Sensing, 48, 365–382, https://doi.org/10.5721/EuJRS20154821, 2015.

Dorren, L.: Rockyfor3D (v6.0) revealed – Transparent description of the complete 3D rockfall model, ecorisQ, https://www.ecorisq.org, ecorisQ manual, 2024.

Edelmann, P., Weisser, W. W., Ambarlı, D., Bässler, C., Buscot, F., Hofrichter, M., Hoppe, B., Kellner, H., Minnich, C., Moll, J., Persoh, D., Seibold, S., Seilwinder, C., Schulze, E.-D., Wöllauer, S., and Borken, W.: Regional variation in deadwood decay of 13 tree species: Effects of climate, soil and forest structure, Forest Ecology and Management, 541, 121 094, https://doi.org/10.1016/j.foreco.2023.121094, 2023.

Feistl, T., Bebi, P., Teich, M., Bühler, Y., Christen, M., Thuro, K., and Bartelt, P.: Observations and modeling of the braking effect of forests on small and medium avalanches, Journal of Glaciology, 60, 124–138, https://doi.org/10.3189/2014JoG13J055, 2014.

Fuhr, M., Bourrier, F., and Cordonnier, T.: Protection against rockfall along a maturity gradient in mountain forests, Forest Ecology and Management, 354, 224–231, https://doi.org/10.1016/j.foreco.2015.06.012, 2015.

Getzner, M., Gutheil-Knopp-Kirchwald, G., Kreimer, E., Kirchmeir, H., and Huber, M.: Gravitational natural hazards: Valuing the protective function of alpine forests, Forest Policy and Economics, 80, 150–159, https://doi.org/10.1016/j.forpol.2017.03.015, 2017.

Gossner, M. M., Wende, B., Levick, S., Schall, P., Floren, A., Linsenmair, K. E., Steffan-Dewenter, I., Schulze, E.-D., and Weisser, W. W.: Deadwood enrichment in European forests – Which tree species should be used to promote saproxylic beetle diversity?, Biological Conservation, 201, 92–102, https://doi.org/10.1016/j.biocon.2016.06.032, 2016.

Harmon, M., Franklin, J., Swanson, F., Sollins, P., Gregory, S., Lattin, J., Anderson, N., Cline, S., Aumen, N., Sedell, J., Lienkaemper, G., Cromack, K., and Cummins, K.: Ecology of coarse woody debris in temperate ecosystems, in: Advances in Ecological Research, vol. 15 of *Advances in Ecological Research*, pp. 133–302, Academic Press, https://doi.org/10.1016/S0065-2504(08)60121-X, 1986.

Herrmann, S., Kahl, T., and Bauhus, J.: Decomposition dynamics of coarse woody debris of three important central european tree species, Forest Ecosystems, 2, https://doi.org/10.1186/s40663-015-0052-5, 2015.

Holeksa, J., Zielonka, T., and Żywiec, M.: Modeling the decay of coarse woody debris in a subalpine Norway spruce forest of the West Carpathians, Poland, Canadian Journal of Forest Research, 38, 415–428, https://doi.org/10.1139/X07-139, 2008.

Kemper, J. T. and Scamardo, J.: Snow avalanches as a driver of large wood dynamics in mountain streams, Geophysical Research Letters, 50, 1 – 11, https://doi.org/10.1029/2023GL106355, 2023.

Lachat, T., Brang, P., Bolliger, M., Bollmann, K., Brändli, U.-B., Bütler, R., Herrmann, S., Schneider, O., and Wermelinger, B.: Totholz im Wald: Entstehung, Bedeutung und Förderung, Merkblatt für die Praxis, 52, 2014.

Leine, R. I. and van de Wouw, N.: Stability and Convergence of Mechanical Systems with Unilateral Constraints, Springer Berlin Heidelberg, ISBN 9783540769750, https://doi.org/10.1007/978-3-540-76975-0, Lecture Notes in Applied and Computational Mechanics, 2008.

https://doi.org/10.5194/egusphere-2026-130
Preprint. Discussion started: 24 March 2026
© Author(s) 2026. CC BY 4.0 License.

Leine, R. I., Schweizer, A., Christen, M., Glover, J., Bartelt, P., and Gerber, W.: Simulation of rockfall trajectories with consideration of rock shape, Multibody System Dynamics, 32, 241–271, https://doi.org/10.1007/s11044-013-9393-4, 2014.

Leverkus, A. B., Polo, I., Baudoux, C., Thorn, S., Gustafsson, L., and Rubio de Casas, R.: Resilience impacts of a secondary disturbance: Meta-analysis of salvage logging effects on tree regeneration, Journal of Ecology, 109, 3224–3232, https://doi.org/10.1111/1365-2745.13581, 2021.

Lu, G., Ringenbach, A., Caviezel, A., Sanchez, M., Christen, M., and Bartelt, P.: Mitigation effects of trees on rockfall hazards: does rock shape matter?, Landslides, 18, 59–77, https://doi.org/10.1007/s10346-020-01418-2, 2021.

Marangon, D., Betetto, C., Wohlgemuth, T., Cadez, L., Alberti, G., Tomelleri, E., and Lingua, E.: Impact of salvage logging on short-term natural regeneration in montane forests of the Alps after large windthrow events, Forest Ecology and Management, 567, 122 085, https://doi.org/10.1016/j.foreco.2024.122085, 2024.

Maser, C. and Trappe, J. M.: The seen and unseen world of the fallen tree, General technical report pnw-164, U.S. Department of Agriculture, Forest Service, Pacific Northwest Forest and Range Experiment Station, 1984.

May, C. L. and Gresswell, R. E.: Large wood recruitment and redistribution in headwater streams in the southern Oregon coast range, USA., Canadian Journal of Forest Research, 33, 1352–1362, https://doi.org/10.1139/x03-023, 2003.

Mayer, M., Rosinger, C., Gorfer, M., Berger, H., Deltedesco, E., Bässler, C., Müller, J., Seifert, L., Rewald, B., and Godbold, D. L.: Surviving trees and deadwood moderate changes in soil fungal communities and associated functioning after natural forest disturbance and salvage logging, Soil Biology and Biochemistry, 166, 108 558, https://doi.org/10.1016/j.soilbio.2022.108558, 2022.

Moos, C., Dorren, L., and Stoffel, M.: Quantifying the effect of forests on frequency and intensity of rockfalls, Natural Hazards and Earth System Sciences, 17, 291–304, https://doi.org/10.5194/nhess-17-291-2017, 2017.

Noël, F., Cloutier, C., Jaboyedoff, M., and Locat, J.: Impact-Detection Algorithm That Uses Point Clouds as Topographic Inputs for 3D Rockfall Simulations, Geosciences, 11, https://doi.org/10.3390/geosciences11050188, 2021.

Oberle, B., Milo, A. M., Myers, J. A., Walton, M. L., Young, D. F., and Zanne, A. E.: Direct estimates of downslope deadwood movement over 30 years in a temperature forest illustrate impacts of treefall on forest ecosystem dynamics, Canadian Journal of Forest Research, 46, 351–361, https://doi.org/10.1139/cjfr-2015-0348, 2016.

Olschewski, R., Bebi, P., Teich, M., Wissen Hayek, U., and Grêt-Regamey, A.: Avalanche protection by forests — A choice experiment in the Swiss alps, Forest Policy and Economics, 15, 108–113, https://doi.org/10.1016/j.forpol.2011.10.002, 2012.

Petrillo, M., Cherubini, P., Fravolini, G., Marchetti, M., Ascher-Jenull, J., Schärer, M., Synal, H.-A., Bertoldi, D., Camin, F., Larcher, R., and Egli, M.: Time since death and decay rate constants of Norway spruce and European larch deadwood in subalpine forests determined using dendrochronology and radiocarbon dating, Biogeosciences, 13, 1537–1552, https://doi.org/10.5194/bg-13-1537-2016, 2016.

Piazza, N., Bebi, P., Vacchiano, G., Rigling, A., Wohlgemuth, T., and Bottero, A.: Post-windthrow forest development in spruce-dominated mountain forests in Central Europe, Forest Ecology and Management, 561, 121 884, https://doi.org/10.1016/j.foreco.2024.121884, 2024.

Plath, E. and Fischer, K.: Spruce dieback as chance for biodiversity: Standing deadwood promotes beetle diversity in post-disturbance stands in western Germany, Journal of Insect Conservation, 28, 525–537, https://doi.org/10.1007/s10841-024-00571-6, 2024.

Rackelmann, F., Sebesvari, Z., and Bell, R.: Synergies and trade-offs in the management objectives forest health and flood risk reduction, Frontiers in Forests and Global Change, 6, https://doi.org/10.3389/ffgc.2023.1208032, 2023.

Rammig, A., Fahse, L., Bebi, P., and Bugmann, H.: Wind disturbance in mountain forests: Simulating the impact of management strategies, seed supply, and ungulate browsing on forest succession, Forest Ecology and Management, 242, 142–154, https://doi.org/10.1016/j.foreco.2007.01.036, 2007.

https://doi.org/10.5194/egusphere-2026-130
Preprint. Discussion started: 24 March 2026
© Author(s) 2026. CC BY 4.0 License.

Ringenbach, A., Bebi, P., Bartelt, P., Rigling, A., Christen, M., Bühler, Y., Stoffel, A., and Caviezel, A.: Modeling deadwood for rockfall mitigation assessments in windthrow areas, Earth Surface Dynamics, 10, 1303–1319, https://doi.org/10.5194/esurf-10-1303-2022, 2022a.

Ringenbach, A., Stihl, E., Bühler, Y., Bebi, P., Bartelt, P., Rigling, A., Christen, M., Lu, G., Stoffel, A., Kistler, M., Degonda, S., Simmler, K., Mader, D., and Caviezel, A.: Full-scale experiments to examine the role of deadwood in rockfall dynamics in forests, Natural Hazards and Earth System Sciences, 22, 2433–2443, https://doi.org/10.5194/nhess-22-2433-2022, 2022b.

Ringenbach, A., Bebi, P., Bartelt, P., Rigling, A., Christen, M., Bühler, Y., Stoffel, A., and Caviezel, A.: Shape still matters: rockfall interactions with trees and deadwood in a mountain forest uncover a new facet of rock shape dependency, Earth Surface Dynamics, 11, 779–801, https://doi.org/10.5194/esurf-11-779-2023, 2023.

Rocscience Inc.: RocFall3: Rigid-body dynamics theory manual, Rocscience Inc., https://www.rocscience.com/help/rocfall3/verification-theory/theory-manuals, accessed 10 Dec 2025, 2024.

Schönenberger, W., Noack, A., and Thee, P.: Effect of timber removal from windthrow slopes on the risk of snow avalanches and rockfall, Forest Ecology and Management, 213, 197–208, https://doi.org/10.1016/j.foreco.2005.03.062, 2005.

Seidl, R., Thom, D., Kautz, M., Martin-Benito, D., Peltoniemi, M., Vacchiano, G., Wild, J., Ascoli, D., Petr, M., Honkaniemi, J., Lexer, M. J., Trotsiuk, V., Mairota, P., Svoboda, M., Fabrika, M., Nagel, T. A., and Reyer, C. P. O.: Forest disturbances under climate change, Nature Climate Change, 7, 395–402, https://doi.org/10.1038/nclimate3303, 2017.

Stadelmann, G., Bugmann, H., Wermelinger, B., and Bigler, C.: Spatial interactions between storm damage and subsequent infestations by the European spruce bark beetle, Forest Ecology and Management, 318, 167–174, https://doi.org/10.1016/j.foreco.2014.01.022, 2014.

Studer, C. W.: Augmented Time-Stepping Integration of Non-Smooth Dynamical Systems, Ph.D. thesis, ETH Zurich, https://doi.org/10.3929/ETHZ-A-005556821, 2008.

swisstopo: swissALTI3D (2023), swissSURFACE3D (2020), SWISSIMAGE (2022), swissMAP Raster 10 (2024), https://www.swisstopo.admin.ch/en, last accessed: 2024-07-01, 2020–2024.

Wermelinger, B.: Ecology and management of the spruce bark beetle Ips typographus—a review of recent research, Forest Ecology and Management, 202, 67–82, https://doi.org/10.1016/j.foreco.2004.07.018, 2004.

Yan, P., Zhang, J., Kong, X., and Fang, Q.: Numerical simulation of rockfall trajectory with consideration of arbitrary shapes of falling rocks and terrain, Computers and Geotechnics, 122, 103 511, https://doi.org/10.1016/j.compgeo.2020.103511, 2020.